

Sensitivity and Specificity of Metal Surface-Immobilized “Molecular Beacon” Biosensors

Hui Du,[†] Christopher M. Strohsahl,[§] James Camera,[†] Benjamin L. Miller,^{*,‡,§} and
Todd D. Krauss^{*,†}

*Contribution from the Department of Dermatology, Department of Biochemistry and Biophysics,
Department of Chemistry, and The Center for Future Health, University of Rochester,
Rochester, New York*

Received December 14, 2004; E-mail: krauss@chem.rochester.edu; Benjamin_Miller@futurehealth.rochester.edu

Abstract: The separate developments of microarray patterning of DNA oligonucleotides, and of DNA hairpins as sensitive probes for oligonucleotide identification in solution, have had a tremendous impact on basic biological research and clinical applications. We have combined these two approaches to develop arrayable and label-free biological sensors based on fluorescence unquenching of DNA hairpins immobilized on metal surfaces. The thermodynamic and kinetic response of these sensors, and the factors important in hybridization efficiency, were investigated. Hybridization efficiency was found to be sensitive to hairpin secondary structure, as well as to the surface distribution of DNA hairpins on the substrate. The identity of the bases used in the hairpin stem as well as the overall loop length significantly affected sensitivity and selectivity. Surface-immobilized hairpins discriminated between two sequences with a single base-pair mismatch with high sensitivity (over an order of magnitude difference in signal) under identical assay conditions (no change in stringency). This represents a significant improvement over other microarray-based techniques.

Introduction

Microarray technology has revolutionized the field of molecular biology and is playing a significant role in both basic research and clinical genomic studies. Applications for microarray technology are numerous and include pathogen detection, high-throughput medical diagnostics, gene expression profiling, drug discovery, and counter bioterrorism.^{1–7} Finding ways to improve the speed, simplicity, and sensitivity of microarray experiments is a continuing challenge for the scientific community. Considerable efforts have been made to reduce background signals and improve data replication,⁸ to develop highly specialized arrays for accurate diagnosis,⁹ and to optimize probe design and sensitivity.¹⁰ Typically, microarray formats employ linear single-strand DNA probes for capturing targets in hybridization reactions.^{7,11} One shortcoming of this approach

is that it requires target labeling, which costs time, money, and can increase the potential for errors in the analysis due to additional steps.

An alternative approach is to use detection schemes based on DNA hairpins. The use of DNA hairpins as “molecular beacons”¹² in solution^{13–17} has proven to be a useful method for “label-free” detection of oligonucleotides. Molecular beacons consist of DNA hairpins functionalized at one terminus with a fluorophore and at the other with a quencher. In the absence of their complement, they exist in a closed, “dark” conformation. Hybridization occurs upon introduction of complementary oligonucleotides, which concomitantly forces open the hairpin and allows for a fluorescent, “bright” state. DNA hairpins have been found to exhibit extraordinary stability, better selectivity, and higher specificity than similar assays performed using single-stranded DNA.^{18,19} An example of the high specificity exhibited by DNA hairpins has been demonstrated by their ability to reliably discriminate single base-pair mismatched

[†] Department of Chemistry.

[§] Department of Biochemistry and Biophysics.

[‡] Department of Dermatology.

- (1) Yoo, S. M.; Keum, K. C.; Yoo, S. Y.; Choi, J. Y.; Chang, K. H.; Yoo, N. C.; Yoo, W. M.; Kim, J. M.; Lee, D.; Lee, S. Y. *Biotech. Bioprocess Eng.* **2004**, *9*, 93–99.
- (2) Gracey, A. Y.; Cossins, A. R. *Annu. Rev. Physiol.* **2003**, *65*, 231–259.
- (3) Guo, Q. M. *Curr. Opin. Oncol.* **2003**, *15*, 36–43.
- (4) Fan, J.; Yang, X.; Wang, W.; Wood, W. H., III; Becker, K. G.; Gorospe, M. *Proc. Natl. Acad. Sci., U.S.A.* **2002**, *99*, 10611–10616.
- (5) Fang, Y.; Frutos, A. G.; Lahiri, J. *Langmuir* **2003**, *19*, 1500–1505.
- (6) Schfering, M.; Kruschina, M.; Meerkamp, M.; Ortigao, F.; Kambhampati, D. *PharmaGenomics* **2002**, September/October, 36–44.
- (7) Pirrung, M. C. *Angew. Chem., Int. Ed.* **2002**, *41*, 1276–1289.
- (8) Donovan, D. M.; Becker, K. G. *J. Neurosci. Methods* **2002**, *118*, 59–62.
- (9) Sawiris, G. P.; Sherman-Baust, C. A.; Becker, K. G.; Cheadle, C.; Teichberg, D.; Morin, P. J. *Cancer Res.* **2002**, *62*, 2923–2928.
- (10) Vainrub, A.; Pettitt, B. M. *J. Am. Chem. Soc.* **2003**, *125*, 7798–7799.

- (11) Heller, M. J. *Annu. Rev. Biomed. Eng.* **2002**, *4*, 129–153.
- (12) Broude, N. E. *Trends Biotech.* **2002**, *20*, 249–256.
- (13) Dubertret, B.; Calame, M.; Libchaber, A. *J. Nat. Biotech.* **2001**, *19*, 365–370.
- (14) Tyagi, S.; Kramer, F. R. *Nat. Biotech.* **1996**, *14*, 303–308.
- (15) Joshi, H. S.; Tor, Y. *Chem. Commun.* **2001**, 549–550.
- (16) Heinlein, T.; Knemeyer, J. P.; Piester, O.; Sauer, M. *J. Phys. Chem. B* **2003**, *107*, 7957–7964.
- (17) Vet, J. A. M.; Majithia, A. R. M.; Marras, S. A. E.; Tyagi, S.; Dube, S.; Poiesz, B. J.; Kramer, F. R. *Proc. Natl. Acad. Sci., U.S.A.* **1999**, *96*, 6394–6399.
- (18) Williams, D. J.; Hall, K. B. *Biochemistry* **1996**, *35*, 14665–14670.
- (19) Riccelli, P. V.; Merante, F.; Leung, K. T.; Bortolin, S.; Zastawny, R. L.; Janeczko, R. and Benight, A. S. *Nucleic Acid Res.* **2001**, *29*, 996–1004.

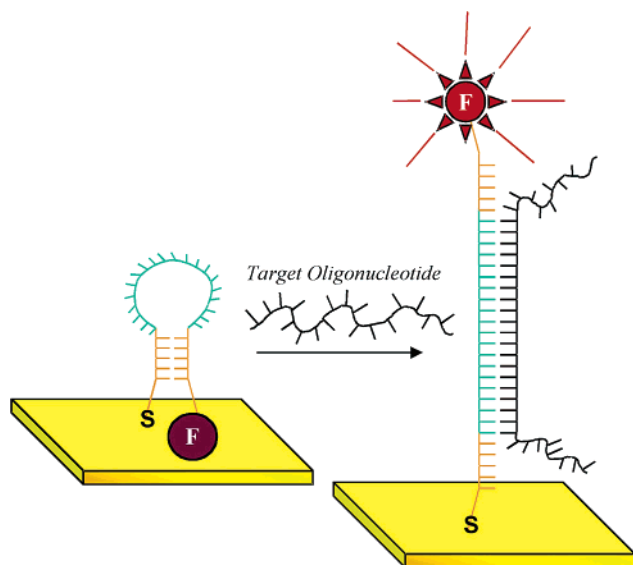


Figure 1. Working principle of the DNA sensor.

targets.¹³ The use of DNA hairpins that contain protein-binding domains has also been recently proposed, thus allowing for potential applications in protein detection.^{20,21} Besides solution phase use, DNA hairpin probes have been immobilized onto solid substrates, including optical fiber surfaces,^{22,23} and glass slides.^{24,25} However, in these studies, the substrates served only as an anchor: the function of the probe was unchanged from the solution assays.

Recently, our groups²⁶ and others²⁷ have investigated whether the substrate itself can serve as a more efficient quenching agent for a surface-immobilized molecular beacon. The operational scheme of our fluorescence unquenching approach is depicted in Figure 1. An oligonucleotide modified with a thiol or thioether at its 5' end is self-assembled onto a gold substrate. The oligonucleotide is designed in such a way that, in the absence of complementary DNA, the oligonucleotide will fold onto itself forming a hairpin loop that is stable in buffered saline at room temperature. In this case, the fluorophore at the 3' end will be brought in close proximity to the gold surface, and its fluorescence will be quenched by the gold through a resonance energy transfer or "contact quenching" process. Upon hybridization to a complementary sequence, the hairpin stem is opened and the dye is separated from the gold, resulting in the restoration of its fluorescence. The overall fluorescence intensity recorded from all the photoexcited dye molecules reflects the extent of the hybridization process.

Hybridization of nucleic acid targets with immobilized DNA probes is the central event in the solid-phase-based detection of nucleic acids. For linear DNA probes, immobilization has been found to impact hybridization in a variety of ways. For

example, surface probe density dependent kinetics and/or steric constraints may alter the apparent stability or selectivity of probe-target binding for surface immobilized oligonucleotides.^{28,29} The major factors that affect hybridization have also been extensively investigated for solution phase molecular beacons.^{30,31} Several studies^{19,23,32} have focused on the in situ kinetics and thermodynamics for surface immobilized hairpin probes interacting with solution-phase targets, which is presumably a more complex process. These three studies (refs 19, 23, and 32) all employed avidin-biotin chemistry to immobilize the beacon on a surface; we can anticipate that our direct-binding scheme will have significantly altered kinetic or thermodynamic behavior.

In this paper we present measurements of the thermodynamic and kinetic behavior of surface-immobilized DNA probes and examine the factors important in determining their hybridization efficiency. We found that the hybridization efficiency is very sensitive to probe secondary structural features, as well as to probe surface distribution on the substrate. A judicious choice of nucleotides for the probe stem and overall loop length will give higher signal-to-noise ratios and larger discrimination factors for specific vs nonspecific targets. We also investigated the specificity of the probe through total mismatch and single-base mismatch tests and found that high specificity (by over an order of magnitude in signal) could be obtained with no changes in assay stringency.

When considering the applicability of any novel biological sensor for bioanalyses, it is important that a "proof of principle" be demonstrated on a range of naturally occurring analytes. This condition is even of higher importance when considering sensors for the rapid identification of harmful organisms. To that end, our hairpin probes (H1 and H2) were designed to match portions of the *Staphylococcus aureus femA* and *mecR* methicillin-resistance genes, respectively. Our studies were not limited to the aforementioned sequences, however. Thus far, we have demonstrated similar device performance using *naturally occurring hairpin probes* discovered in the genes of *Bacillus anthracis* and *Staphylococcus aureus*.³³ On the basis of these results, we expect that the surface-immobilized molecular beacon concept will be generally applicable.

Experimental Section

Materials. The oligonucleotide sequences for both the probes and targets are shown in Table 1. All oligonucleotides were purchased from Midland Certified Reagent Co. Oligonucleotide probes were functionalized at the 5' end with a thiol group and at the 3' end with tetramethylrhodamine (TMR). 3-Mercapto-1-propanol was purchased from Aldrich chemical company and used without further purification. All H₂O used in the preparation of buffers and for rinse solutions had a resistivity of 18.2 MΩ cm, as produced by a Barnstead Nanopure system. The buffered saline used was 0.5 M NaCl, 20 mM Cacodylic acid, and 0.5 mM EDTA, pH = 7.

- (20) Dai, X.; Greizerstein, M. B.; Nadas-Chinni, K.; Rothman-Denes, L. B. *Proc. Natl. Acad. Sci., U.S.A.* **1997**, *94*, 2174–2179.
 (21) Heyduk, T.; Heyduk, E. *Nat. Biotech.* **2002**, *20*, 171–176.
 (22) Steemers, F. J.; Ferguson, J. A.; Walt, D. R. *Nat. Biotech.* **2000**, *18*, 91–94.
 (23) Liu, X.; Tan, W. *Anal. Chem.* **1999**, *71*, 5054–5059.
 (24) Piester, O.; Barsch, H.; Buschmann, V.; Heinlein, T.; Knemeyer, J. P.; Weston, K. D.; Sauer, M. *Nano Lett.* **2003**, *3*, 979–982.
 (25) Fang, X.; Liu, X.; Schuster, S.; Tan, W. *J. Am. Chem. Soc.* **1999**, *121*, 2921–2922.
 (26) Du, H.; Disney, M. D.; Miller, B. L.; Krauss, T. D. *J. Am. Chem. Soc.* **2003**, *125*, 4012–4013.
 (27) Fan, C.; Plaxco, K. W.; Heeger, A. J. *Proc. Natl. Acad. Sci., U.S.A.* **2003**, *100*, 9134–9137.

- (28) (a) Satjapipat, M.; Sanedrin, R.; Zhou, F. *Langmuir* **2001**, *17*, 7637–7644.
 (b) Grunwell, J. R.; Glass, J. L.; Lacoste, T. D.; Deniz, A. A.; Chemla, D. I. S.; Schultz, P. G. *J. Am. Chem. Soc.* **2001**, *123*, 4295–4303.
 (29) Georgiadis, R. M.; Peterlinz, K. P.; Peterson, A. W. *J. Am. Chem. Soc.* **2000**, *122*, 3166–3173.
 (30) Aalberts, D. P.; Parman, J. M.; Goddard, N. L. *Biophys. J.* **2003**, *84*, 3212–3217.
 (31) Bonnet, G.; Libchaber, A. *Physica A* **1999**, *263*, 68–77.
 (32) Yao, G.; Fang, X.; Yokota, H.; Yanagida, T.; Tan, W. *Chem.—Eur. J.* **2003**, *9*, 5686–5692.
 (33) Strohsahl, C. M.; Du, H.; Krauss, T. D.; Miller, B. L., in preparation.

Table 1. DNA Hairpin Probes and Their Targets

name	sequence
H1 (probe)	5'-(-C6Thiol) ACACGCTCATCATAACCTTCAGCAAGCTTTAACTCATAGTGAGCGTGT (-3'Amino C7) (TMR)-3'
H2 (probe)	5'-(-C6Thiol) AATGATGATAACACCTTCTACACCTCCATAATCATCATT (-3'Amino C7) (TMR)-3'
H3 (probe)	5'-(-C6Thiol) ACACGCTCATCAAGCTTTAACTCATAGTGAGCGTGT (-3'Amino C7) (TMR)-3'
T1 (H1 complement)	5'-ACGCTCACTATGAGTTAAAGCTTGCTGAAGGTTATGA-3'
T2 (H2 complement)	5'-TATGGAGGTGTAGAAGGTTATCATCATT-3'
T3 (H3 complement)	5'-ACGCTCACTATGAGTTAAAGCTTG-3'
T3M1 (single mismatch of H3)	5'-ACGCTCACTATGAGTTAAAGCTTG-3'

DNA Melting Experiments. The computer program RNAStructure v. 3.7³⁴ was used to predict the secondary structure of all DNA probes. The lowest-energy structures were predicted using parameters derived from ref 35. Thermal melting experiments were performed on all sequences, on a Gilford spectrophotometer, with the oligonucleotide dissolved in buffered saline. Each sample was warmed to 80 °C, and then cooled back to 10 °C prior to running the melting experiments. Melting temperatures were found to be independent of concentration for the hairpin probes, thus proving a unimolecular conformational transition in solution as predicted.²⁶ For the probe-target duplex, melting temperatures were concentration dependent, thus supporting the formation of a duplex under target invasion.²⁶

Preparation of Substrate and DNA Immobilization. Glass slides were cleaned with piranha etch solution (4:1 concentrated H₂SO₄/30% H₂O₂) overnight at room temperature and then rinsed with ultrapure water. Metal deposition was performed at a rate of 0.2 nm/s using a Denton Vacuum Evaporator (DV-502A). First, a chromium adhesion layer of 7 nm was coated on the glass, followed by a 100 nm thick gold film. Before use, the gold substrates were annealed at 200 °C for 4 h and cleaned with piranha solution for 0.5–1 h.

The self-assembly process consisted of soaking the gold substrate in a mixture of hairpin oligonucleotide and mercaptopropanol. Two hours later, the substrate was thoroughly rinsed with hot water (90 °C or higher) to remove any nonbonded DNA. Rinsing the gold after self-assembly is an important step; otherwise, some probe molecules will attach to the bottom of the cover slip causing a large background signal, since TMR has a strong interaction with glass and is easily adsorbed.³⁶ Next, the substrate carrying the mixed monolayer was immersed in buffered saline for hairpin formation. Hybridization to the hairpin probes on the gold was performed at room temperature under the same conditions.

Surface Probe Density Measurement. To determine the amount of probe hairpin immobilized per unit area, we prepared a substrate containing unlabeled H1 as the probe. A labeled version of T1 (T1-Rhodamine) was used as the target. After hybridization, nonbound target was removed by rinsing with buffered saline at room temperature. The target-probe duplex was then unhybridized by heating to >80 °C in 1.5 mL of Nanopure water. The resultant solutions were then analyzed by fluorescence spectroscopy for the presence of the fluorophore. Comparison to a standard curve yielded the quantity of the target, from which the surface density of the probe on the substrate was derived.

Single-Mismatch Tests in Solution. Molecular beacons (H3 in Table 1) modified with a 5'-Fluorescein and a 3'-Dabsyl and either their full complement (T3), or one containing a single base mismatch (T3M1) were taken up in hybridization buffer to a final volume of 1 mL. The concentration of beacon was held constant at 300 nM, while the concentration of both the complement and the mismatch was varied from 300 to 1200 nM. Samples were kept out of direct light as much as possible prior to excitation to prevent photo bleaching. Measurements of fluorescence intensity were performed with excitation at 470 nm in a 1.0 cm path length quartz cuvette. The resulting optical emission spectrum was monitored from 470 to 620 nm.

(34) Mathews, D. H.; Sabina, J.; Zuker, M.; Turner, D. H. *J. Mol. Biol.* **1999**, *288*, 911–940.

(35) SantaLucia, J., Jr. *Proc. Natl. Acad. Sci., U.S.A.* **1998**, *95*, 1460–1465.

(36) Maxwell, D. J.; Taylor, J. R.; Nie, S. *J. Am. Chem. Soc.* **2002**, *124*, 9606–9612.

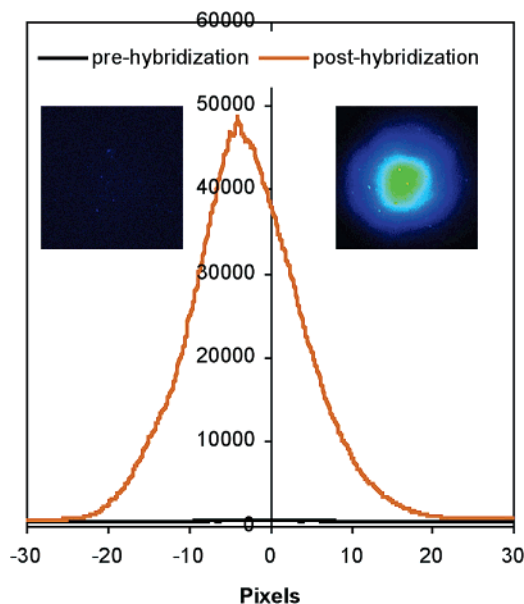


Figure 2. Fluorescence of the chip with H1 as probe and T1 as target. The intensity data is derived from binning the CCD fluorescence images before (left inset) and after (right inset) hybridization.

Fluorescence Detection. Fluorescence measurements from immobilized molecular beacons were performed on a Nikon inverted microscope equipped with a liquid nitrogen cooled charge-coupled device (CCD) as reported in ref 26. The substrate was inverted, and excitation was at 514 nm through a 0.85 NA, 60× air objective. Light was collected through the same objective and passed through a dichroic beam splitter, a holographic notch filter (Kaiser Optical, Inc.), and a band-pass filter (585 ± 5 nm, ensuring only fluorescence from Rhodamine was observed) and imaged with the CCD. To track the fluorescence of a certain area, a pattern was scratched on the gold so that exactly the same area could be examined before and after hybridization. At least four areas at different positions of one gold chip were chosen for each sample during a given fluorescence measurement. While under laser illumination, the fluorescence intensity was observed to irreversibly decay with time, likely due to photobleaching of the dye molecule.²⁶ To mitigate the effects of photobleaching, images were recorded at intensities less than 20 W/cm² with a 10-s integration time.

The fluorescence intensity of a particular area was obtained through binning all the counts of the laser spot in that area. The relative increase in the fluorescence intensity after hybridization was calculated as: $R = (I_{\text{target}} - I_{\text{blank}}) / (I_{\text{probe}} - I_{\text{blank}})$, where I_{probe} is the fluorescence intensity of hairpin probe on gold before hybridization, I_{target} is the fluorescence intensity of hairpin probe on gold after hybridization with the target sequences, and I_{blank} is the fluorescence intensity of background including bare gold, cover slip and buffer.

Results

A typical result for the chip with H1 as the probe is shown in Figure 2. The two inset pictures are CCD images of the chip under laser illumination before (left) and after (right) incubation

Table 2. Relationship of MP:DNA Ratio and the Fluorescence Increase Fold R in Eq 1 (DNA (H1) Concentration (0.13 μM))

sample no.	ratio of MP:DNA	prehybridization intensity	posthybridization intensity	R
1	0:1	4084	2981	0.73
2	1:1	3683	5636	1.53
3	5:1	1778	9123	5.13
4	10:1	506	11992	23.7
5	20:1	297	579	1.95
6	30:1	184	344	1.87

in the complementary target T1 solution. After binning the intensity of each pixel from the CCD images along the y -axis, we obtained the curves in Figure 2. The difference between pre- and post-hybridization can be clearly seen and the fluorescence intensity was increased as high as 100 fold.

Effect of Modifying Surface Density of DNA Probes.

Preparation of the DNA chip involves immersion of the Au substrate in a solution containing the probe. By control of the exposure time and concentration of probes in the solution, one is able to obtain the desired probe density. Intuitively, one would imagine that an ever-increasing density of surface bound probes would lead to an increasingly better chip performance. However, this is not the case. The single-strand probes used in this study are fairly long sequences (48mer or 39mer for H1 and H2, respectively), so it is possible for them to lie flat, wrap together, or even to form duplexes if the local surface density is high enough.³⁶ All these situations will prevent the probes from forming hairpin loops and thus lead to poor fluorescence quenching and a high background. Additionally, other studies of hybridization to surface-immobilized probe oligonucleotides have found that some interstitial space between probes is necessary for high hybridization efficiency.^{37,38,39,40}

Two strategies were used to control the surface coverage of probe DNA. Initially, we used a relatively low concentration of DNA (131 nM) in solution and a short incubation time (less than 2 h). However, poor quenching of fluorescence before hybridization was observed, and an alternative strategy for controlling probe surface density was sought. Thus, we varied the coverage of surface-bound DNA by forming a two-component monolayer consisting of thiolated DNA and 3-mercaptopropanol (MP) which served as a spacer. MP was used as the blocking molecule since its short carbon chain will not interfere with the hybridization reactions of the surface-bound hairpin. Using the mixed monolayer to control surface coverage was critical. We assume that MP assists in two ways. First, the use of MP potentially provides sufficient space between probes such that hairpin loops were formed and hybridization could occur. Second, the presence of MP potentially reduces the number of noncovalent interactions between the DNA backbone and the gold by preventing the nitrogen-containing nucleotide bases from interacting directly with the Au surface.³⁸

Table 2 shows the dependence of fluorescence intensity after hybridization vs the ratio of MP to DNA probe H1 with T1 as the target. The surface density of DNA in the mixed monolayer

was varied with different ratios between MP and hairpin DNA from 1:1 to 50:1. As seen in the table, too little MP results in high background fluorescence, and thus a small difference in signal between pre- and post-hybridization. Too much MP results in too low a probe density on the surface, which leads to a low fluorescence intensity after hybridization. A ratio of 10:1 gave the best performance.

We attempted to measure the surface probe density by hybridizing unlabeled H1 and TMR labeled T1 under conditions identical to the actual assay. The ratio of MP to H1 was fixed at 10:1. After hybridization, the probes on the chip were denatured and the amount of T1-Rhodamine was determined by comparing the fluorescence intensity to a standard curve.⁴⁰ Peterson et al.⁴¹ and Dodge et al.⁴² reported that on a solid surface a perfectly matched target can bind with 100% efficiency. Thus, we assume that when the hybridization reaches the saturation point approximately all probes have hybridized. In our experiments, we used a large excess of target (2.5 μM , 300 μL) and incubated for a very long time (at least 5 h) to make sure that hybridization reached the saturation point. We varied the concentration of probe solutions for assembly on the surface from 100 to 800 nM, and looked for a corresponding probe surface density difference. Our results show that the hairpin probe coverage is $\sim 10^{12}$ molecules/cm² for all cases. This value is similar to linear single-strand DNA probe densities (10^{12} – 10^{13} molecules/cm²) used in commercial microarrays⁷ and other experiments^{32,40,41} on hybridization investigations of surface immobilized linear single strand DNA probes.

Input Target Concentration Studies. Concentration of the complementary target sequences plays an important role in hybridization efficiency. Figure 3 shows the relative fluorescence increase (normalized R in eq 1) from the chip vs the concentration of perfectly matched target. Low concentrations of the target resulted in weak fluorescence, whereas at higher concentrations the dye fluorescence increased in a highly nonlinear fashion (Figure 3). The measured line shape does not agree even qualitatively with a simple 1:1 solution-phase binding model described by $\theta = [P]/([P]+K_d)$,⁴³ where θ is the fraction of hybridized probes, $[P]$ is the free target concentration, and K_d is the dissociation constant for the duplex (See Figure 3). In fact, the good agreement with a sigmoidal line shape (Figure 3) indicates that the fluorescence signal is essentially “off” or “on” (i.e., a two-state system) and thus implies that duplex formation is highly cooperative. Such behavior is not unprecedented, as both Jin et al.⁴⁴ and Sauthier et al.³⁹ found a nonlinear relationship between DNA hybridization efficiency and target concentration for oligomer-labeled gold nanoparticles and gold substrates, respectively. Although a probe density of ~ 1 molecule/(100 nm²) is not especially high (which would favor cooperativity), the cooperative effect we observe could arise if the distribution of hairpin probes on the gold surface is not homogeneous. For example, some areas might be much denser locally than others, which may result in a clustering together due to a bonding between probes. Fluorescence is only

(37) Pena, S. R.; Raina, S.; Goodrich, G. P.; Fedoroff, N. V.; Keating, C. D. *J. Am. Chem. Soc.* **2002**, *124*, 7314–7323.

(38) Gearheart, L. A.; Ploehn, H. J.; Murphy, C. J. *J. Phys. Chem. B* **2001**, *105*, 12609–12615.

(39) Sauthier, M. L.; Carroll, R. L.; Gorman, C. B.; Franzen, S. *Langmuir* **2002**, *18*, 1825–1830.

(40) Lin, Z.; Strother, T.; Cai, W.; Cao, X.; Smith, L. M. and Hamers, R. J. *Langmuir* **2002**, *18*, 788–796.

(41) (a) Peterson, A. W.; Wolf, L. K.; Georgiadis, R. M. *J. Am. Chem. Soc.* **2002**, *124*, 14601–14607. (b) Peterson, A. W.; Heaton, R. J.; Georgiadis, R. M. *Nucleic Acids Res.* **2001**, *29*, 5163–5168.

(42) Dodge, A.; Turcatti, G.; Lawrence, I.; Rooij, N. F.; Verpoorte, E. *Anal. Chem.* **2004**, *76*, 1778–1787.

(43) Weeks, K. M.; Crothers, D. M. *Biochemistry* **1992**, *31*, 10281–10287.

(44) Jin, R.; Wu, G.; Li, Z.; Mirkin, C. A.; Schatz, G. C. *J. Am. Chem. Soc.* **2003**, *125*, 1643–1654.

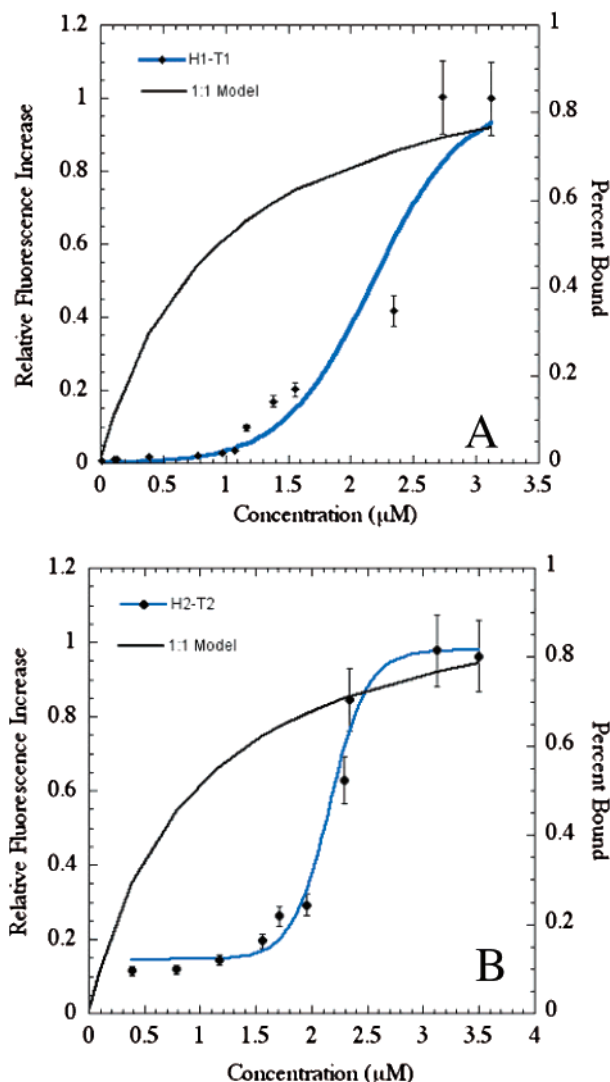


Figure 3. Relative fluorescence enhancement ratio of the two pairs of probe-target as a function of the input complementary target concentration for sequence H1 (a) and H2 (b). Solid black line is based on a simple 1:1 binding model $\theta = [P]/([P] + K_d)$, where θ is the fraction of hybridized probes, $[P]$ is the free target concentration and K_d is the dissociation constant for the duplex. For the calculation, K_d is $0.95 \mu\text{M}$. The solid blue line is a theoretical fit based on a two-state model given by $R = (R_0 + R_F(e^{\alpha-\beta[P]})^{-1}) / (1 + (e^{\alpha-\beta[P]})^{-1})$, where R_0 and R_F are the initial and final normalized relative fluorescence intensities and α and β are adjustable parameters. The values used for the calculation for H1-T1 are $R_0 = 0.0$, $R_F = 1.0$, $\alpha = 6.1$, and $\beta = 2.8$, and for H2-T2 are $R_0 = 0.15$, $R_F = 0.98$, $\alpha = 12.7$, and $\beta = 5.7$.

observed when enough targets are present to open the whole “cluster” of hairpins, which would produce the trend shown in Figure 3. Also, other areas would naturally have a low probe concentration resulting at low concentration of target binding to the gold, which also would not result in a fluorescence signal. Thus, only after a critical target concentration will all the probes unfold and give a restoration of fluorescence. Indeed, during fluorescence detection, we typically found that some areas of the chip were brighter than others for the same laser power, implying that the probe distribution is not homogeneous. Also, atomic force microscopy (AFM) measurements in water of attached hairpin probe/MP monolayers on the gold surface show many domains of higher and lower regions on the surface, likely corresponding to clustered areas of DNA probes (Figure 1S of Supporting Information). It is unclear how we would reconcile this “clustering” with the need for a specific 10:1 MP:DNA

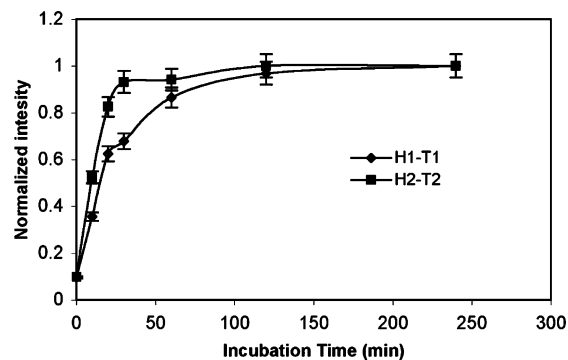


Figure 4. Hybridization kinetics of two probes on gold surface. Concentrations of T1 and T2 are 2.34 and $2.73 \mu\text{M}$, respectively.

ratio. Additional experiments designed to examine the relationship of coassembled thiol:DNA probe, observation of surface domain structure, and chip function are in progress.

Hybridization Kinetics of the Hairpin Probes on the Chip.

The kinetics of hairpin invasion by the target were analyzed by monitoring the fluorescence intensity as a function of incubation time. Figure 4 illustrates the results obtained for H1-T1: a rapid initial hybridization rate was observed that monotonically slowed over time. We found a 50% maximal relative fluorescence increase was obtained in approximately 15 min of incubation with target, and steady state was reached in less than 2 h.

H2-T2 reaches a 50% maximal relative fluorescence increase in approximately 10 min and reaches its saturation point in about 30 min, which is much shorter than was found for H1-T1. Since H1 (calculated $\Delta G_{37} = -7.2$ kcal/mol, measured $T_m = 69$ °C) is more stable than H2 (calculated $\Delta G_{37} = -4.3$ kcal/mol, measured $T_m = 58$ °C), the higher activation barrier to the open configuration likely slows the hybridization kinetics. Also, it has been shown that the presence of secondary structure of the target decreases the hybridization rate.⁴⁵ T1 is predicted to form a more stable loop structure than T2 (Figure 2s in Supporting Information), which is consistent with the kinetic data. Steric hindrance could also account for the differences in hybridization kinetics between H1-T1 and H2-T2. H1 has nine nucleotides more than H2 and thus potentially needs more “space” for duplex formation. Since in our case the DNA probes are immobilized on a substrate surface, sterics play a much more important role in the hairpin invasion process than for free hairpin probes in solution. This idea was recently demonstrated by Peterson et al.⁴¹ who investigated the surface hybridization kinetics of linear DNA for different lengths and different surface densities. It was found that longer DNA targets and higher probe surface densities significantly retarded duplex formation due to steric crowding. Additionally, the faster hybridization kinetics for H2-T2 could also partially result from the slightly higher concentration of T2 used in the experiment ($2.34 \mu\text{M}$ for T1 vs $2.73 \mu\text{M}$ for T2).

Binding Specificity in DNA Probe Hybridization. To evaluate the binding specificity of the hairpin probes on the gold substrate, we ran a control experiment with a noncomplementary target. Two chips incubated with H1 were prepared at the same time. One was exposed to T1, and the other was exposed to T2. As shown in Figure 5a, for H1-T1, the

(45) Kushon, S. A.; Jordan, J. P.; Seifert, J. L.; Nielsen, H.; Nielsen, P. E.; Armitage, B. A. *J. Am. Chem. Soc.* **2001**, *123*, 10805–10813.

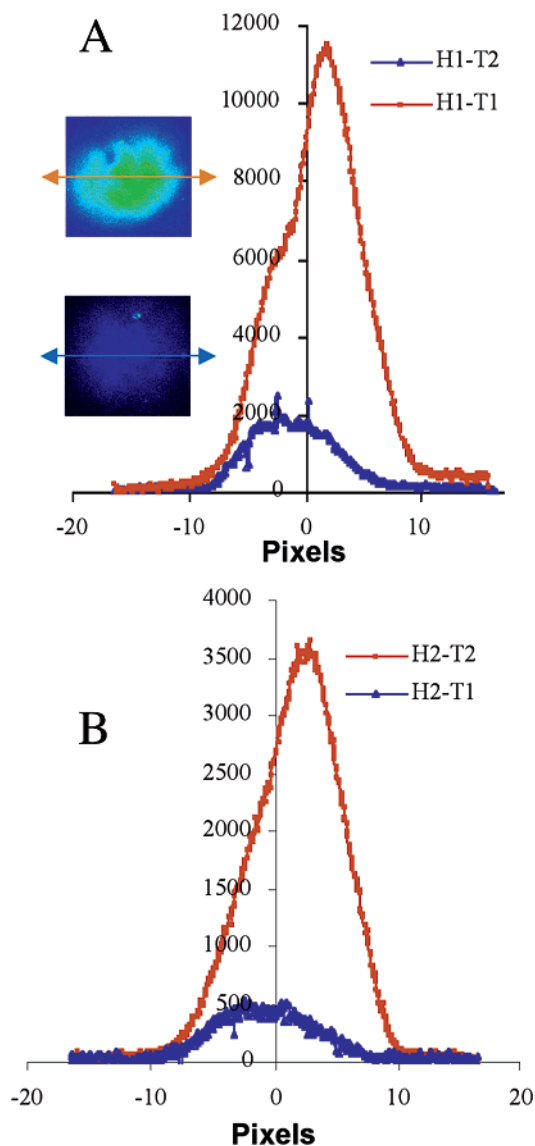


Figure 5. Comparison of binding between complementary target and total mismatch target for sequence H1 (a) and H2 (b) at the same concentrations. The curves are binned fluorescence counts from the CCD images. (Top inset) CCD fluorescence image of H1–T1. (Bottom inset) CCD fluorescence image of H1–T2. All curves are background (prehybridization) subtracted.

fluorescence intensity increased by a factor of 20, while H1–T2 only showed a 3-fold increase. A similar experiment was performed for substrates using H2 as probes. As indicated in Figure 5b, H2–T2 produces a 6-fold more intense fluorescence signal than H2–T1. Calculations indicate that sequence T2 can form six base pairs with H1 and that T1 can form eight base pairs with H2 (Figure 3s in Supporting Information). Thus, some limited unquenching of dye fluorescence by the totally mismatched targets is not surprising. Although some fluorescence was observed on mismatched targets, as expected, the fluorescence signal was much stronger for the complementary sequences than for the mismatched ones.

Detection of Single-Base Mismatch DNA. The ability to distinguish single-base mismatches is the gold standard of DNA-targeted detection, and part of the appeal of solution-phase molecular beacons has been their high performance in this regard.¹³ To test for single mismatch discrimination, we employed a 36-mer hairpin probe H3 and two 24-mer targets,

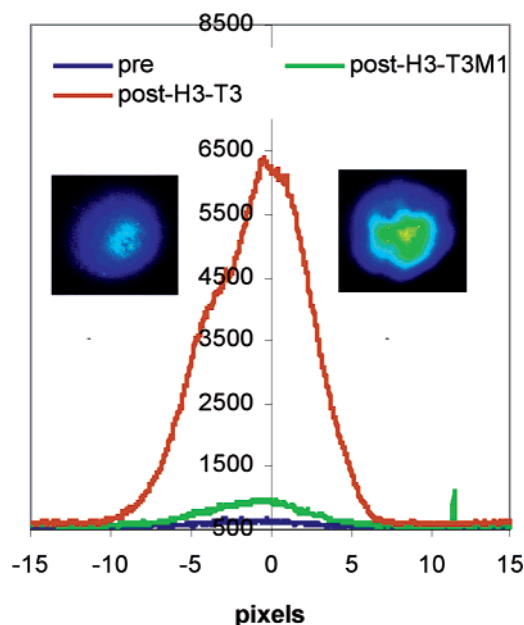


Figure 6. Single mismatch discrimination using probe H3. The fluorescence intensity curves are binning data of the CCD images after hybridization. The concentration of both T3 and T3M1 is 2 μ M. (Right inset) CCD fluorescence image of H3–T3. (Left inset) CCD fluorescence image of H3–T3M1.

where T3M1 has one G–G mismatch compared with the complementary sequence T3. Two chips containing surface-immobilized H3 were prepared at the same time and then were respectively incubated into the perfect target and the mismatch target solutions of equal concentration. Figure 6 shows the fluorescence CCD images as well as the binned images after hybridization. An 8-fold weaker fluorescence signal occurs for the single mismatched target compared with the complement. A fluorescence intensity comparison for both targets at concentrations ranging from 1.18 μ M to 2.6 μ M is shown in Figure 7a. In general, the overall signal for both the match and single mismatch increases with target concentration due to the increased signal enhancement for target concentrations above 2 μ M (Figure 3). The mismatch discrimination also increases with target concentration, likely because (at a given concentration above threshold) the less efficient hybridization of the single mismatch is less able to trigger a cooperative response than the perfect match.

Since hybridization parameters on substrate surfaces may differ from simple solution-based duplex formation, we performed experiments using the same probe sequences and targets, (H3 binding to T3M1 and T3) as described above except in solution with “traditional” molecules as quenching agents, and in lower overall concentrations. Our results, shown in Figure 7b, demonstrate that H3 can discriminate single base mismatched targets effectively both as a solution-phase hairpin probe and in its surface-immobilized form. Interestingly, the maximum match-mismatch discrimination on the chip is substantially greater than in solution. While it appears that surface immobilization increases specificity, it is difficult to quantitatively assign a relative contribution to the selectivity of just the probe due to the dramatically different hybridization environments for the surface vs solution phase assay.

Our single base-pair mismatch results are consistent with what one would predict based on thermodynamic considerations. The

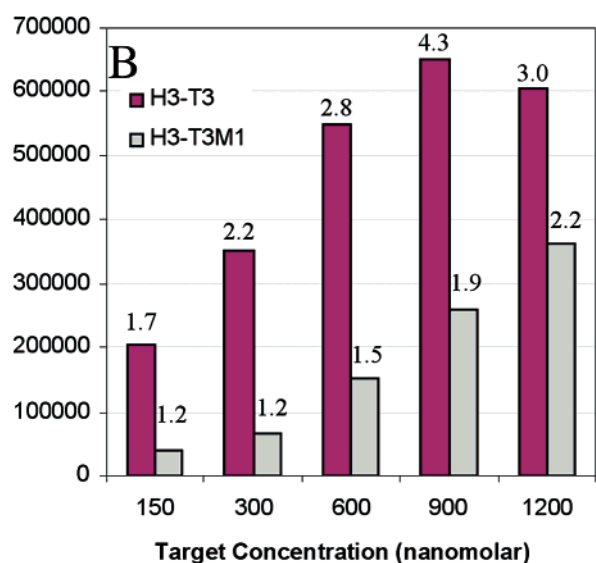
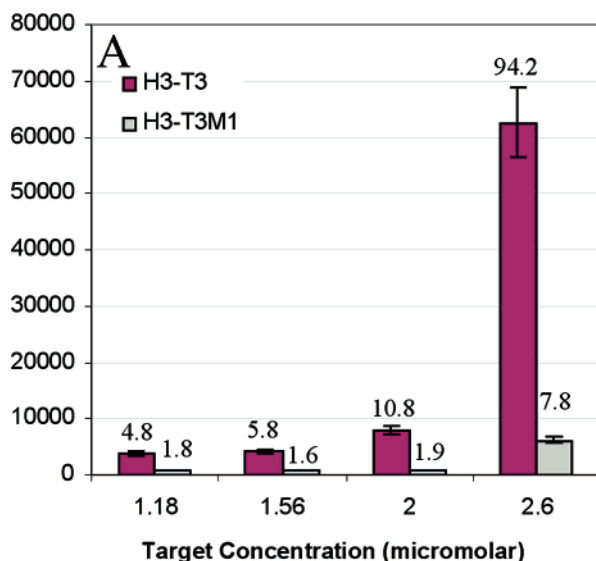


Figure 7. Hybridization of hairpin probe H3 on chip (a) and in solution (b) with perfect match T3 and single-mismatch T3M1 as a function of target concentration. Prehybridization (background) fluorescence has been subtracted in each case. Numerical values over the bars indicate fold increase relative to background.

difference of binding energy (predicted with RNA Structure v.3.7³⁴) for a duplex between H3–T3 and H3–T3M1 is 6.9 kcal/mol. Thermal melting experiments show that single mismatched targets form a duplex in solution with a melting temperature $\sim 2\text{--}3$ °C lower than the perfect matched duplex. Thus, one would expect that the increased stability of the duplex for the perfect match relative to the single-base mismatch would translate into more efficient hybridization and thus a stronger signal. Of note is that, although the difference in binding energy between the match and the mismatch is smaller than the norm,⁴¹ the surface-immobilized beacon was still able to discriminate between the match and mismatch with high sensitivity, thus demonstrating high specificity.

Single mismatch discrimination with DNA probes immobilized on gold nanoparticles has been reported previously with a 4- to 25-fold difference in signal between the complements and mismatch.^{13,46,47} However, in these experiments the reaction conditions (temperature or ionic strength) were biased

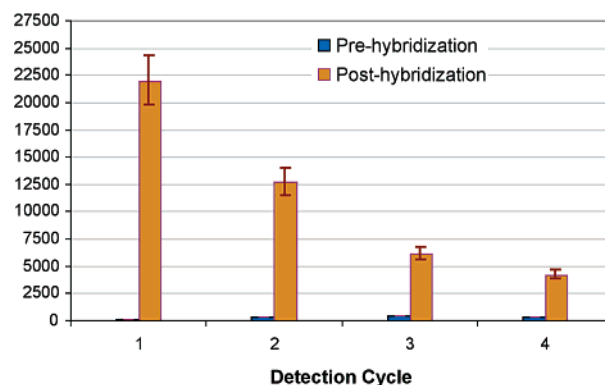


Figure 8. Multiple recycle use of the chip. The fluorescence intensity of the chip was obtained through binning the CCD images before and after hybridization.

such that unlike the complement, the mismatched duplex would not be energetically stable. Using unfavorable reaction conditions for the mismatch is commonly referred to as changing the stringency of the assay or a stringency test. In our case, hybridization takes place under identical reaction conditions for both the perfect match and the mismatched target, which allows for a more realistic comparison between responses to a perfectly complementary target, or one containing a single base mismatch. Since the parameters that control hybridization (for example free-energy change) depend on target concentration, the high sensitivity to single base-pair mismatches may result from the particular concentration range we used here. While this idea is possible, the high selectivity observed over the wide range of concentrations used for the immobilized and solution-phase studies suggests that the molecular beacon itself fundamentally provides for a highly selective assay.

Reusability of the Chip. Reusability of a particular device is a desired feature for some biosensor applications. We tested the ability to reuse the DNA chip by regenerating the original state of the hairpin probes thermally. Specifically, after the first hybridization process, the substrate was rinsed with 90 °C water to denature the duplex and then immersed in buffer at room temperature to refold the probe hairpins. The regenerated chip was incubated in the target DNA and after the usual workup produced a fluorescence signal in the presence of the target, demonstrating the regeneration of the sensor. Figure 8 shows the relative response for four regenerative cycles of one chip. As expected, the fluorescence intensity of the chip decreases with repeated regenerative cycles, decreasing by 40% (1–13075 counts/22410 counts), another 50% (1–6533 counts/13075 counts), and another 30% (1–4603 counts/6533 counts) for cycles 2, 3, and 4, respectively. We attribute the decrease in response to loss of probe molecules from the chip surface during heating and rinsing.

The probe loss we observed is similar to that reported when other approaches for binding DNA probes to glass or silicon substrates are employed. Dodge et al.⁴² modified a Si wafer with (3-aminopropyl) aminotriethoxysilane and then bound thiolated DNA through a cross-linker sulfo-MBS. Ramachandran et al.⁴⁸ attached molecular beacons containing a primary amino group to the surface of aldehyde-modified glass via the

(46) Taton, T. A.; Mirkin, C. A.; Letsinger, R. L. *Science* **2000**, *289*, 1757–1760.

(47) Storhoff, J. J.; Elghanian, R.; Mucic, R. C.; Mirkin, C. A. *J. Am. Chem. Soc.* **1998**, *120*, 1959–1964.

formation of a Schiff base. In both these cases, the loss of probes was always observed. Better surface chemistry is needed to improve the immobilization of probes on substrates for enhanced reusability of the chip.

Discussion

Probe selection is important since it is critical for determining hybridization efficiency and thus chip performance.⁴⁹ Under similar hybridization conditions the conformation of a molecular beacon will be determined by the competition between the hairpin configuration and the duplex. Since the free energy of duplex formation is much more favorable than that of hairpin formation, the duplex forms, which results in the restoration of fluorescence. However, the chip performance does not only depend on the signal intensity but also on the signal-to-noise ratio, which improves with lower background fluorescence. Naturally, a higher signal-to-noise ratio is desired for any analytical method to reduce errors and eliminate false responses. As reported by Tyagi et al.¹⁴ and Tan et al.,⁵⁰ a six-pair stem is long enough to form a stable hairpin in solution. However, in our case we chose an eight- to nine-pair stem for better selectivity and quenching efficiency on the surface.

Most molecular beacon studies indicate that an excellent balance between selectivity and sensitivity is achieved with 15–25 loop nucleotides together with a 5–7-base-pair stem.⁵⁰ Our studies using H1 (a 48-mer) show that well-designed longer probes on surfaces can also achieve such a balance. Indeed, optimization of assembly and detection conditions can result in relative fluorescence increases of over 2 orders of magnitude upon hybridization with the complementary target (Figure 2). Such a high relative increase in fluorescence intensity is far superior to what is typically observed for other immobilized molecular beacons, which show enhancements of 2–25-fold as reported.^{22,25,42,48,51}

Interestingly, probe H2 (a 39-mer) did not exhibit the same level of relative signal enhancement as H1: the relative fluorescence signal increased by a factor of 16. The smaller enhancement suggests that the performance of the chip is very sensitive to the primary and secondary structural features of the molecular beacon probe, and thus specific applications will need corresponding specific probe designs. For example, longer probes will be favorable for higher sensitivity due to the formation of a more thermodynamically stable duplex but may also be more tolerant and therefore less discriminatory to single-base mismatches. Shorter probes, on the other hand, are capable of displaying faster hybridization kinetics during real-time detection but may not have optimal sensitivity.⁵⁰ Although we have not thoroughly tested all possible loop and stem permutations, our results suggest that both stem and probe lengths and sequences must be carefully chosen for best performance. We are currently studying how the presence of internal secondary structure elements affect beacon performance.

Single-base mismatches are the most common form of genetic polymorphisms and can often be used to diagnose particular genetic predispositions toward disease and drug response.

Several groups have worked on single mismatch discrimination. In solution, Hwang et al.⁵² observed a discrimination factor of 14.7 at a single A/C mismatch using a quencher-free molecular beacon that contains fluorine deoxyuridine derivative. Higher discrimination ratios of 25 were obtained by Dubertret et al.¹³ using gold nanoparticle hairpin DNA dye conjugates in solution phase under stringency conditions. For molecular beacon assays on a solid surface, the specific/nonspecific signal ratios obtained^{23,42,53} are in the range of only 2–6. By comparison, our surface immobilized beacons can distinguish a G/G mismatch out of a 24-base-pair target at room temperature with a discrimination ratio ranging between 2- and 12-fold. There have been limited investigations^{19,23,30} on the hybridization process of immobilized molecular beacons interacting with solution phase targets, and on the molecular level this complex process is still not well understood. Some studies^{40,41} indicate for surface immobilized linear oligonucleotides the probe density and steric constraints may alter the apparent stability or selectivity of probe-target binding. In our experiment, the overall probe density is order of 10^{12} molecules/cm²; however, AFM measurements show that the distribution of probes is likely not uniform likely introducing steric constraints during hybridization.

Molecular beacons have been demonstrated to have many advantages for real time detection.^{54–56} They can detect target hybridization without separation of the hybridized and nonhybridized probes, and the target DNA is label free, which means many laborious and costly procedures can be eliminated. For example, our detection methodology will be able to detect methicillin-resistant *S. aureus* (MRSA) genes reliably within 20 minutes, with the maximum signal available in only 2 h. Compared with traditional pathogen diagnostics,⁵⁷ this new detection methodology could ultimately provide a guide to the appropriate therapies a full 24–36 h earlier than has been previously possible. The value of being able to rapidly and reliably identify pathogenic organisms increases exponentially when the difference between a treatable infection and a lethal infection can be measured in hours, as would be the case in the event of a biological weapons release.

Sensitivity is an important issue of DNA sensing technology. For our design, an increase of fluorescence can be observed when the chip is incubated in as low as 10 nM target. With a target concentration lower than this, some spots on the chip show a fluorescence increase and some areas do not. Improvements in control of the probe surface density and uniformity may help to solve this problem. Also, currently hybridization takes place in a relatively large volume vessel. Designing a high aspect ratio container optimized for surface binding should increase sensitivity significantly. Sensitivity can also be improved through reducing the background signal coming from the optics, getting better quenching by rough metal surface and enhancing the fluorescence through the plasmon resonance.

(48) Ramachandran, A.; Flinchbaugh, J.; Ayoubi, P.; Olah, G. A.; Malayer, J. R. *Biosens. Bioelectron.* **2004**, *19*, 727–736.

(49) Tsourkas, A.; Behlke, M. A.; Rose, S. D.; Bao, G. *Nucleic Acids Res.* **2003**, *31*, 1319–1330.

(50) Tan, W.; Fang, X.; Li, J.; Liu, X. *Chem.—Eur. J.* **2000**, *6*, 1107–1111.

(51) Culha, M.; Stokes, D. L.; Griffin, G. D.; Vo-Dinh, T. *Biosens. Bioelectron.* **2004**, *19*, 1007–1012.

(52) Hwang, G. T.; Seo, Y. J.; Kim, B. H. *J. Am. Chem. Soc.* **2004**, *126*, 6528–6529.

(53) Frutos, A. G.; Pal, S.; Quesada, M.; Lahiri, J. *J. Am. Chem. Soc.* **2002**, *124*, 2396–2397.

(54) Elsayed, S.; Chow, B. L.; Hamilton, N. L.; Gregson, D. B.; Pitout, J. D. D.; Church, D. L. *Arch. Pathol. Lab. Med.* **2003**, *127*, 845–849.

(55) Tang, Z. W.; Wang, K. M.; Tan, W. H.; Li, J.; Liu, L. F.; Guo, Q. P.; Meng, X. X.; Ma, C. B.; Huang, S. S. *Nucleic Acid Res.* **2003**, *23*, e148.

(56) Perlette, J.; Tan, W. H. *Anal. Chem.* **2001**, *73*, 5544–5550.

(57) Versalovic, J. *Arch. Pathol. Lab. Med.* **2003**, *127*, 784–785.

Conclusions

We developed a DNA sensor based on a surface-immobilized molecular beacon hybridization format. The hairpin probes were self-assembled on gold substrate, which acts as a quencher. By control of the ratio of MP to DNA probe and rinsing after self-assembly, signals from the chip can be optimized. After hybridization with complementary targets, the fluorescence signal can increase more than 100-fold. Kinetic studies suggest that strong while hairpin structure influences the rate at which maximum signal is obtained from the chip, a significant fluorescence intensity can be observed in less than 15 min. Target concentration influences the hybridization efficiency, and a more complimentary target sequence can trap the hairpin probe in an open configuration resulting in a higher fluorescence signal. Total mismatch and single mismatch tests demonstrate the excellent selectivity of the hairpin probes. The chip is in principle reusable, but loss of probes was observed, most likely due to the high-temperature washing process during duplex

dehybridization, which limits practical reusability. It is anticipated that optimization of surface chemistry will lead to improvements in sensor stability.

Acknowledgment. The authors acknowledge useful discussions with Douglas Turner and assistance with equipment from Brent Znosko. This work was supported by the New York Office of Science, Technology, and Academic Research, and the Department of Energy through an award to the New York State Infotonics Technology Center (DE-FG02-02ER63410.A000).

Supporting Information Available: AFM images of the bare Au substrate and the DNA hairpin/MP monolayer on Au, secondary structure predictions of all hairpins and targets, and secondary structure predictions of possible duplexes formed between hairpins and mismatched targets. This material is available free of charge via the Internet at <http://pubs.acs.org>.

JA042482A